

An MILP framework for gas supply chain infrastructure planning with endogenous logistics schemes



Yoga Wienda Pratama ^{a,b,c,*¹}, Nadhilah Reyseliani ^{b,c}, Widodo Wahyu Purwanto ^{b,c}

^a Energy, Climate, and Environment Program, International Institute for Applied Systems Analysis (IIASA), Laxenburg, 2361, Austria

^b Department of Chemical Engineering, Faculty of Engineering, Universitas Indonesia, Depok, 16424, Indonesia

^c Sustainable Energy Systems and Policy Research Cluster (SESP), Universitas Indonesia, Depok, 16424, Indonesia

ARTICLE INFO

Keywords:

Liquefied natural gas
Optimisation
Supply chain design
Mixed-integer linear programming

ABSTRACT

This paper presents a mixed-integer linear programming (MILP) framework to minimise the costs of gas supply chains. Distinct from existing approaches in the literature, which often rely on pre-defined logistics schemes and treat storage sizing at receiving terminals in isolation, this framework integrates these into a single optimisation model. By setting these elements as decision variables, the framework allows for simultaneous optimisation of shipping strategies and receiving terminals design. Here, the liquefied natural gas (LNG) supply chain in Indonesia's Maluku Islands was used as a case study. Additionally, the framework was applied to the Finnish coastline and the Caribbean Islands, which differ substantially in terms of demand levels, distances between locations, and geographical contexts, to demonstrate its applicability to problems with differing characteristics. The results show that clustering demands to increase project sizes can lead to significant cost reductions. However, the marginal gains of these economies of scale diminish rapidly as project size grows, especially with longer shipping distances. Finally, the proposed framework was also shown to provide substantially lower-cost solutions compared to methods that rely on pre-determined shipping strategies or optimise shipping and storage capacities separately.

1. Introduction

Climate change mitigation requires rapid increases in the utilisation of cleaner energy sources. In this context, gaseous fuels, such as natural gas and hydrogen, are expected to play a significant role in phasing out carbon-intensive fuels, such as coal and oil (Abdin, 2024; Intergovernmental Panel on Climate Change IPCC, 2023; Reyseliani et al., 2024; Spatolisano et al., 2024). Natural gas is widely regarded as a key in energy system transitions over the coming decades, especially in developing regions that must balance climate mitigation ambitions with financial, infrastructure, and institutional constraints (Bugaje et al., 2022; Pratama and Mac Dowell, 2022; Raza and Lin, 2022). Hydrogen, on the other hand, can serve as a clean energy carrier when produced from renewables, which are often geographically constrained (Faydi et al., 2024; Olabi et al., 2023; Pratama et al., 2017).

Despite their potential, transporting those fuels over long distances to areas with small and dispersed demands tends to be costly due to the

lack of economies of scale (Nekså et al., 2010; Ratnakar et al., 2021). To address this, separate demand sites are served together via a partial unloading strategy (Bittante et al., 2018). This approach compensates for the absence of unit-level economies of scale on the demand side by increasing project or system size, allowing more efficient use of shared facilities (Bai and Fan, 2023; Pratama et al., 2024), such as shipping facilities, to reduce costs. Accordingly, systems modelling and optimisation become increasingly important tools for integrated supply chain infrastructure designs and planning to minimise the plant gate costs, i.e., the final cost of natural gas delivered to end-users.

As can be seen in Table 1, several frameworks and models were developed for this purpose, with the number and size of carriers, shipping routes, and fuel suppliers typically incorporated as decision variables. Several studies, such as in (Bai and Fan, 2023; Bittante et al., 2018; Budiyanto et al., 2020), disregarded storage sizing for receiving terminals, focusing exclusively on the shipping costs by assuming that sufficient storage capacity is already installed in receiving terminals or

This article is part of a special issue entitled: Advancement in Gas Production and Storage published in Gas Science and Engineering.

* Corresponding author. Energy, Climate, and Environment Program, International Institute for Applied Systems Analysis (IIASA), Laxenburg, 2361, Austria.

E-mail address: pratama@iiasa.ac.at (Y.W. Pratama).

¹ Lead contact.

Table 1

Overview of existing supply chain design approaches in the literature. The symbols (X) and (O) in the table indicate that the model element is treated as a parameter or a decision variable, respectively. If neither symbol is present, the element is not included in the model.

Source	Methods	Temporal resolution		Design parameters												Note	
				Supply and demand		Storage size of terminals		Logistic scheme			Shipping strategy		Objective function				
		Single-period	Multi-period	Supply	Demand	Exporting	Receiving	Point-to-point	Milk-and-run	Hub-and-spoke	Ship routes	Number/type	System cost	Environmental impact	Risk factor	Utilisation factor	
Machfudiyanto et al. (2023)	Genetic Algorithm	X		X		O		X			O	X	O		O		-
Jokinen et al. (2015)	MILP		X	O		O		O			O	O	O				-
Bittante and Saxén (2020)	MILP	X	X	O		O	O	O			O	O	O				Compared multi-period and single-period optimisations
Bittante et al. (2018)	MILP	X		O				O	O		O	O	O				-
Santos and Guedes Soares (2024)	MILP		X	O		X		O			O	O			O		-
Al-Haidous et al. (2022)	MILP		X	O		O		O	O		O	O	O	O	O		Storage inventory levels at the exporting terminals are included as constraints
Doymus et al. (2022)	MILP		X	X				O	O		O	O	O				To optimise LNG bunkering. Therefore, there is no storage at delivery locations
Hadi et al. (2023)	Genetic Algorithm	X		X		O		X			X	O	O				-
Abdillah et al. (2021, 2024)	Scenario Analysis					O	X	X			X		O		O		-
Sommeng et al. (2023)	Techno-Economic Analysis		X	X		O		X			X		O		O		-
Budiyanto et al. (2019, 2020, 2022)	Greedy Algorithm	X		X				X	X		X	O	O		O		A greedy algorithm was used to select the optimal design from a predefined set of routes and ship types.
Bai and Fan (2023)	Lagrange Heuristic Algorithm	X		X						O	O	O	O		O		Hub location candidates are preset. A two-stage model was proposed for 1) network design and 2) fleet planning. Implemented for large-scale problems
Eriksen et al. (2022)	MILP	X		O		O		X		O	O	O					Hub location is predetermined, locations are only

(continued on next page)

Table 1 (continued)

Source	Methods	Temporal resolution		Design parameters											Note		
				Supply and demand		Storage size of terminals		Logistic scheme			Shipping strategy		Objective function				
		Single-period	Multi-period	Supply	Demand	Exporting	Receiving	Point-to-point	Milk-and-run	Hub-and-spoke	Ship routes	Number/type	System cost	Environmental impact	Risk factor	Utilisation factor	
Nugroho et al. (2023)	Multiple methods	X		X		X		O	O				O				connected by a point-to-point Compared the Nearest Neighbour, Saving Matrix, and Heuristics methods in solving large-scale problems
Fauzi and Ispandiari (2024)	MILP	X		X		X		O	O		O	O	O				-
Pratiwi et al. (2021)	Techno-Economic Analysis	X		X				O	O		O	O	O				Carriers transport modular storage filled with LNG to receiving terminals and bring back empty storage for refilling.
Papaleonidas et al. (2020)	Genetic Algorithm		X	X				O			O	O	O				Vessel assignment is set as a decision variable for a predetermined route
Strantzali et al. (2018)	Scenario Analysis	X		X		X		O	O		O	O	O	O	O	O	Multi-criteria analysis is performed to evaluate scenarios
This paper	MILP	X		X	X			O	O	O	O	O	O				Shipping routes and hub locations are fully endogenised in the framework

by incorporating existing storage capacity as constraints. This approach simplifies the model and is useful in brownfield cases, *i.e.*, when the storage and regasification facilities in the receiving terminals already exist (Bittante et al., 2018; Jokinen et al., 2015). However, this approach can lead to suboptimal solutions for greenfield designs as storage costs can take a significant portion of the total cost or when the potential shipping cost saving from updating the storage size outweighs the value of avoiding additional storage investments. To address this, some studies incorporated storage sizing as a decision variable, allowing the frameworks to balance shipping, storage, and regasification costs for optimal system designs (Bittante and Saxén, 2020; Eriksen et al., 2022; Hadi et al., 2023; Jokinen et al., 2015).

Despite these efforts, the range of logistic schemes each framework can evaluate remains limited. A range of studies sets the shipping routes exogenously, using only carrier sizing and scheduling as decision variables for the design (Abdullah et al., 2021, 2024; Hadi et al., 2023; Papaleonidas et al., 2020; Sommeng et al., 2023). In large-scale LNG supply systems, the point-to-point schemes, where carriers transport LNG directly from a single supplier to a single consumer, are more popular as the delivery size is already sufficiently large to harness the benefits of the economies of scale effect. The milk-and-run scheme is more common in small-scale LNG supply chains, allowing partial unloading from carriers to serve multiple destinations before returning to the exporting terminal (Bittante et al., 2018; Bittante and Saxén, 2020; Jokinen et al., 2015). In this scheme, carriers collect cargo from an exporting terminal and transport it to several consumers in a single trip. Other logistics scheme options include the hub-and-spoke. In this approach, cargo is transported from the producer to a hub, which will redistribute the commodity to final consumers/destinations. Literature suggests that LNG system design frameworks considering the hub-and-spoke logistic scheme assume point-to-point connections between the hub and final consumers, with hub locations or candidates predetermined (Bai and Fan, 2023; Bittante and Saxén, 2020; Eriksen et al., 2022; Jokinen et al., 2015). Although these approaches simplify the problem and reduce solution time, they might substantially affect the optimal solutions. This is because they restrict the framework from exploring potentially more optimal solutions beyond the predefined scheme and hub locations.

To bridge this gap, a Supply Chain Infrastructure Planning framework (SCIPe) was developed to quantify the impacts of pre-determined shipping strategies and separating shipping and storage sizing optimisations on optimal solutions and costs. The framework comprehensively incorporates shipping fleet sizes, routes, optimal logistic schemes, and storage sizes at receiving terminals. Rather than pre-defining hub locations, logistic schemes, and shipping routes in the system, the proposed framework incorporates these as decision variables. Table 1 compares features of existing frameworks and approaches in the literature with the proposed framework. In this paper, small-scale LNG supply chain designs for the Maluku Islands, the Finnish coastline, and the Caribbean Islands were used as case studies. Here, the proposed framework was applied to these cases, representing systems with different demand levels, distances between locations, and geographical contexts, to demonstrate its applicability to problems with differing characteristics. The results show that the proposed framework can provide lower-cost solutions compared to an approach with predetermined variables. Additionally, it was also observed that supply chain designs with isolated receiving terminals' capacity optimisation can significantly increase costs, potentially negating the benefits of lower shipping costs. Moreover, owing to their small sizes, increasing the project sizes through multiple demands clustering can significantly reduce costs via the economies of scale effect. However, the potential to harness this effect is limited by an increase in shipping distance, which proportionately increases costs.

2. Model description

This paper presents the LNG Supply Chain Infrastructure Planning Framework (LNG-SCIPe), a Mixed Integer Linear Programming (MILP) framework for optimising the design of LNG supply chain systems. The solutions provided by this framework include the number and size of LNG carriers, shipping routes and logistics schemes, the storage capacity at each receiving terminal, as well as the location and storage capacity of LNG hubs. Rather than aiming to provide insights for strategic planning at the enterprise, national, or global level (Fescioglu-Unver and Aktaş, 2023; Garcia and You, 2015; Konstantakopoulos et al., 2022) which typically involves large-scale problems with many node locations, this framework is intended as a tool for project-level supply chain design, where global optimal solutions are required rather than approximate ones (Garcia and You, 2015).

The detailed workflow of the framework is shown in Fig. 1. As can be observed, the model, formulated in General Algebraic Modeling System (GAMS), aims to minimise system cost while considering system-wide constraints, such as LNG demand, supply availability, and the distances between node locations. Unit-level constraints for carrier and storage, including capacity, speed, and loading-unloading rates, are also incorporated. Furthermore, fleet utilisation constraints are included to ensure that a sufficient number of carriers are assigned to each route. The proposed framework uses techno-economic parameters and system data, which are stored in an Excel file, as input. Finally, optimisation results are visualised in Python for the analysis.

Fig. 2 illustrates the possible shipping routes considered in the framework. LNG cargo can be delivered directly from the liquefaction plant to receiving terminals RT1-RT3, using either the point-to-point or milk-and-run schemes, corresponding to carriers' routes 3 and 4, respectively. Alternatively, if more cost-effective, LNG can be transported from the liquefaction plant to receiving terminals (RT4-RT10) via hubs (H1-H3). In this framework, a hub functions similarly to a regular receiving terminal but with larger storage capacity, allowing it to serve as an exporting terminal for smaller terminals. Shipping routes between the liquefaction plant and receiving terminals, the liquefaction plant and hubs, and the hubs and receiving terminals can follow either a point-to-point scheme (solid arrows) or a milk-and-run scheme (dotted arrows). Here, hub locations are optimised and each receiving terminal is assigned to a single exporting terminal, either the liquefaction plant or a hub. This section outlines the mathematical formulation of the proposed framework.

2.1. Objective function

The objective function of this framework, as outlined in Eq. (1), is to minimise the total annual system cost (TASC). This cost includes three components, namely the cost of gas (CoG) at liquefaction plants, the cost of carrier (CoC) for shipping, and the cost of receiving terminals (CoR) for storage and regasification. Here, the subscripts r , i , c , and s denote the shipping route, node location, LNG carrier type, and the storage type at the receiving terminal, respectively.

$$TASC = \sum_{r,i} CoG_{r,i} + \sum_{r,c} CoC_{r,c} + \sum_{i,s} CoR_{i,s} \quad (1)$$

The cost of gas accounts for the free-on-board (FOB) price (pg) and the volume of LNG loaded (Lv) onto carriers (c) for delivery. As can be seen in Eq. (2), a scalar ghv represents gross heating value per volume of LNG. The subscript il , which is a subset of node location i , denotes the location of liquefaction plants. The cost of LNG loading from hubs is not accounted for to avoid double-counting.

$$CoG_{r,il} = \sum_c Lv_{r,c,il} ghv_{il} pg_{il} \quad \forall r, il \in i \quad (2)$$

For each route r , LNG is transported using carriers (c), with the costs of

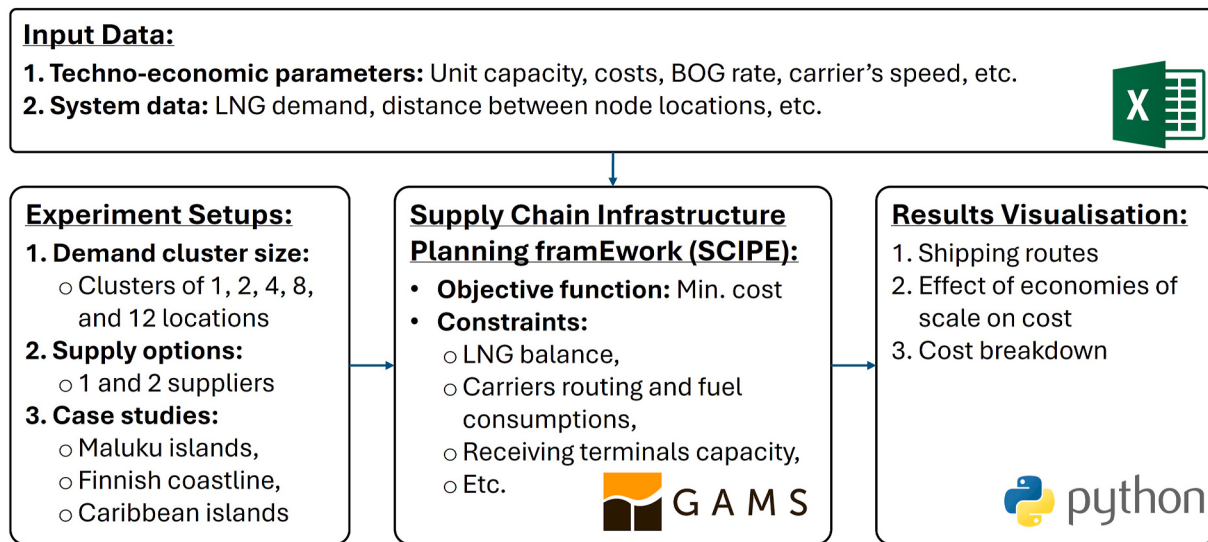


Fig. 1. LNG-SCIE workflow.

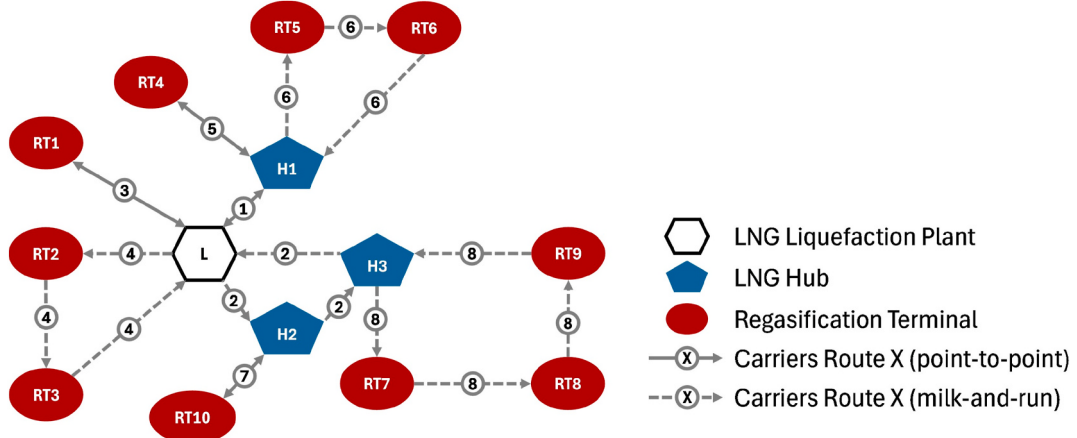


Fig. 2. Illustration of LNG supply systems design from optimisation. The hexagon, pentagon, and oval represent the LNG liquefaction plant, hubs, and receiving terminals, respectively. Arrows indicate the direction of shipping along each route, with the accompanying number denoting the route number. Receiving terminals can receive LNG either directly from the liquefaction plant or via hubs. Hubs function as receiving terminals but can also serve as exporting points, redistributing LNG to other receiving terminals.

owning the fleet being a function of the number (N_c) and type-specific prices (capexc_c) of carriers, annualised using the cost recovery factor (crfc). Additionally, operating and maintenance (O&M) costs are accounted for by including fixed O&M (assumed to be the percentage of the carrier's price, $fomc$) and fuel costs. Fuel costs are calculated based on marine fuel oil (MFO) consumption (Dec), priced at the rate of MFO (pd). These are summarised in Eq. (3), where subscripts j and k denote the ports of origin and destination, respectively.

$$\text{CoC}_{r,c} = N c_{r,c} \text{capexc}_c (\text{crfc} + fomc) + \sum_{j,k} Dec_{r,c,j,k} pd \quad \forall r, c \quad (3)$$

Receiving terminals receive, store, and regasify LNG from carriers. Depending on their type, they may also function as exporting terminals to smaller facilities. In such cases, stored LNG is loaded onto smaller carriers. The costs at receiving terminals (CoR), detailed in Eq. (4), consist of capital expenditures (CAPEX) for storage (capex_s) and non-storage (capexns) components (e.g., the regasification and other utility units), as well as fixed and variable O&M expenses. In this framework, the cost of the non-storage component is modelled as a function of the terminal throughput to local demand (d). Similar to CoC calculations, fixed O&M is assumed as a percentage of capital costs ($fomr$), while

variable O&M pertains to the energy costs for regasification (cgr). Here, S_b , a binary variable representing the storage type installed at the receiving terminal, is incorporated in the equation to assign the regasification cost to the corresponding storage type.

$$\text{CoR}_{i,s} = ((N s_{r,i} \text{capex}_s + S b_{i,s} d_i \text{capexns}_s) (\text{crfr} + fomr) + S b_{i,s} d_i cgr) \quad \forall i, s \quad (4)$$

2.2. Constraints

2.2.1. Carriers routing formulation

To deliver the LNG, shipping strategies are optimised by applying carrier routing constraints. Here, a binary variable (Rb) is introduced to identify active route connections between terminals. Rb is equal to 1 if the route is selected and 0 otherwise. For each route (r), a port of origin (j) can connect to only one port of destination (k). However, at a hub or liquefaction plant where the binary variable Hb equals 1, connections with multiple ports of destination and origin are allowed to serve multiple networks and to refill LNG carriers for onward delivery along the route. This setup is reflected in Eq. (5), where m represents a sufficiently large number. Route connection between ports at the same location is

prohibited (Eq. (6)). Additionally, a binary parameter bi is used in Eq. (7) to exogenously indicate whether a connection between terminals j and k is available for selection. Finally, Eq. (8) ensures continuity of shipping routes, while Eq. (9) enforces that each route is served by either a hub or a liquefaction terminal.

$$\sum_{r,k} Rb_{r,j,k} - Hb_{r,j} m \leq 1 \quad \forall j \quad (5)$$

$$Rb_{r,j,k} = 0 \quad \forall r, j, k = j \quad (6)$$

$$\sum_r Rb_{r,j,k} \leq bi_{j,k} \quad \forall j, k \quad (7)$$

$$\sum_j Rb_{r,j,k} = \sum_j Rb_{r,k,j} \quad \forall r, k \quad (8)$$

$$\sum_j Hb_{r,j} \leq 1 \quad \forall r \quad (9)$$

2.2.2. Ships assignment and fuel consumption

In transporting the LNG, the capacity of carriers is limited by their tank size. Consequently, the annual volume of LNG carried by a carrier, including LNG transported (Tv) and BOG ($Bogv$) volumes, is a function of the frequency of trips (Tr) and the carrier's unit capacity (ucc) (Eq. (10)). Additionally, a fraction of the LNG must remain in the carrier to maintain the cryogenic temperature of its tanks. This volume, known as the "heel", is represented by the heel volume parameter (hvc) in Eq. (11).

$$Tv_{r,c,j,k} + Bogv_{r,c,j,k} \leq Tr_{r,c,j,k} ucc_c \quad \forall r, c, j, k \quad (10)$$

$$Tv_{r,c,j,k} \geq Tr_{r,c,j,k} hvc ucc_c \quad \forall r, c, j, k \quad (11)$$

In this framework, the refilling frequency (Fr) at each receiving terminal is specific to each route. As shown in Eq. (12), the frequency of LNG carriers' trips between origin and destination ports is determined by the product of the binary variable Rb and the route-specific refilling frequency variable (Fr), which introduces a non-linear function. To linearise this, Glover's linearisation method (Glover, 1975) is applied, introducing Eqs. (13)–(17) as equivalent constraints to Eq. (12). In these equations, Fb denotes binary variable to select active route's trip frequency segment (l) while parameters nl and m represent discretised trip frequency and any sufficiently large number, respectively. Additionally, Eq. (18) ensures a minimum trip frequency when a route is selected, preventing a model artifact where a route is selected without a trip being planned, while Eq. (19) ensures trip continuity. Here, Eqs. (20)–(23) ensure that each route operates only one type of carriers, with Cb being the binary variable to select carrier's type.

$$\sum_c Tr_{r,c,j,k} \leq Rb_{r,j,k} Fr_r \quad \forall r, j, k \quad (12)$$

$$Fr_r = \sum_l Fb_{r,l} nl_l \quad \forall r \quad (13)$$

$$\sum_l Fb_{r,l} \leq \sum_i Hb_{r,i} \quad \forall r \quad (14)$$

$$\sum_c Tr_{r,c,j,k} \leq Rb_{r,j,k} m \quad \forall r, j, k \quad (15)$$

$$\sum_c Tr_{r,c,j,k} \leq \sum_l Fb_{r,l} nl_l \quad \forall r, j, k \quad (16)$$

$$\sum_c Tr_{r,c,j,k} \geq \sum_l Fb_{r,l} nl_l - m (1 - Rb_{r,j,k}) \quad \forall r, j, k \quad (17)$$

$$\sum_c Tr_{r,c,j,k} \geq Rb_{r,j,k} \quad \forall r, j, k \quad (18)$$

$$\sum_j Tr_{r,c,j,k} = \sum_j Tr_{r,c,k,j} \quad \forall r, c, k \quad (19)$$

$$Tr_{r,c,j,k} \leq Cb_{r,c} m \quad \forall r, c, j, k \quad (20)$$

$$\sum_c Cb_{r,c} \leq 1 \quad \forall r \quad (21)$$

$$Nc_{r,c} \leq Cb_{r,c} m \quad \forall r, c \quad (22)$$

$$Nc_{r,c} \geq Cb_{r,c} \quad \forall r, c \quad (23)$$

Following this, the number of carriers (Nc) required to serve each network can be quantified by accounting for the time available for carriers to complete their tasks ($avup$). As outlined in Eqs. (24) and (25), the time required by carriers to complete their tasks includes trip durations, which consider the distance between locations and carriers' average speed, and berthing time (btc) for each trip. Additionally, loading and unloading times at terminals, taking into account loading (Lv) and unloading (Uv) volumes as well as the rate ($lurc$), and minimum idle time ($itclo$) allocated for maintenance, schedule safety margins, etc., are also accounted for. Moreover, constraints to ensure minimum utilisation time of carriers ($avlo$) are provided in Eqs. (26) and (27). Eq. (28) assigns a minimum number of LNG carriers to serve each designated hub or liquefaction plant.

$$Nc_{r,c} avup \geq \sum_{j,k} Tr_{r,c,j,k} \left(\frac{di_{j,k}}{vc_c} + btc_c \right) + \sum_k \frac{Uv_{r,c,k}}{lurc_c} + \sum_j \frac{Lv_{r,c,j}}{lurc_c} \quad \forall r, c \quad (24)$$

$$avup = 8760 - itclo \quad (25)$$

$$Nc_{r,c} avlo \leq \sum_{j,k} Tr_{r,c,j,k} \left(\frac{di_{j,k}}{vc_c} + btc_c \right) + \sum_k \frac{Uv_{r,c,k}}{lurc_c} + \sum_j \frac{Lv_{r,c,j}}{lurc_c} \quad \forall r, c \quad (26)$$

$$avlo \leq avup \quad (27)$$

$$\sum_c Nc_{r,c} \geq \sum_j Hb_{r,j} \quad \forall r \quad (28)$$

During each trip, carriers consume marine fuel oil (MFO) and natural gas from BOG formation. The fuel consumption is calculated based on the carrier's fuel economy (fec), the distance between locations in active routes, and the number of trips, which can be seen in Eq. (29). Dec and ghv are MFO consumption and gross heating value of LNG, respectively.

$$Dec_{r,c,j,k} + (Bogv_{r,c,j,k} ghv) = Tr_{r,c,j,k} fec_c di_{j,k} \quad \forall r, c, j, k \quad (29)$$

2.2.3. LNG balance in vessels

In this framework, partial unloading of the LNG at receiving terminals is allowed. Accordingly, the volume of LNG transported (Tv) in shipping network r by carrier c from port j to port k is greater than the volume of LNG unloaded (Uv) at port k plus the remaining volume in the carrier (Rv), as shown in Eq. (30).

$$\sum_j Tv_{r,c,j,k} \geq Uv_{r,c,k} + Rv_{r,c,k} \quad \forall r, c, k \quad (30)$$

Subsequently, the volume of LNG transported to the next destination is less than the remaining volume (Rv) and, if the port of departure is a hub or liquefaction terminal, the volume of LNG loaded onto the carrier (Lv). These volumes are then adjusted for BOG formation during the trip ($Bogv$), outlined in Eq. (31).

$$\sum_k Tv_{r,c,j,k} \leq Rv_{r,c,j} + Lv_{r,c,j} - \sum_k Bogv_{r,c,j,k} \quad \forall r, c, j \quad (31)$$

For each trip, the volume of LNG evaporated as BOG ($Bogv$) depends on the BOG formation rate coefficient ($cbog$), the trip duration, and the volume of LNG being carried (Eq. (32)). Note that a factor of 24 is

applied to account for c_{bog} being specified as a daily rate instead of an hourly rate.

$$Bogv_{r,c,j,k} \geq c_{bog} \frac{d_{j,k}}{24 v_{c_c}} \left(T_{V,r,c,j,k} + Bogv_{r,c,j,k} \right) \quad \forall r, c, j, k \quad (32)$$

Moreover, the volume of LNG a hub can load onto carriers is limited by the volume of LNG it receives (UV), adjusted for the local demand d (Eq. (33)). This constraint does not apply to liquefaction plants il , assuming they always have sufficient LNG production. For each terminal, the LNG must originate from a single supply network (Eqs. (34) and (35)), with the LNG loaded from a terminal designated as the route's hub (Eq. (36)). As can be seen in Eqs. (34) and (35), Uvb is a binary variable that indicates the selected LNG source location for each shipping route.

$$\sum_{r,c} Lv_{r,c,i} \leq \sum_{r,c} Uv_{r,c,i} - d_i \quad \forall i \notin il \quad (33)$$

$$Uv_{r,c,i} \leq Uvb_{r,i} m \quad \forall r, c, i \quad (34)$$

$$\sum_r Uvb_{r,i} \leq 1 \quad \forall i \quad (35)$$

$$Lv_{r,c,i} \leq Hb_{r,i} m \quad \forall r, c, i \quad (36)$$

2.2.4. Storage capacity at receiving terminals

Here, storage capacity (Scr) is represented as the product of the number of units installed (Nsr) and the type-specific capacity per unit (ucs), as can be seen in Eq. (37). LNG delivered by carriers is stored in receiving terminals, where the storage capacity must satisfy a set of volume requirements. First, it must be able to accommodate the volume of LNG unloaded by carriers for each delivery, denoted as $Scur$ in Eq. (38). Second, if the terminal serves as an LNG hub, it must provide sufficient capacity to store LNG for local demand ($Scdr$) and for redistribution to smaller receiving terminals ($Sclr$), as can be seen in Eq. (39). As in Eqs. (16) and (17), the subscript l in Eqs. (38) and (39) denotes discretised segments used to linearise the calculations of $Scur$, $Scdr$, and $Sclr$, which are discussed in more detail in Eqs. (40)–(48).

$$Scr_i \leq \sum_s Nsr_{i,s} ucs_s \quad \forall i \quad (37)$$

$$Scr_i \geq \sum_{r,l} Scur_{r,i,l} \quad \forall i \quad (38)$$

$$Scr_i \geq \sum_{r,l} Scdr_{r,i,l} + \sum_{r,l} Sclr_{r,i,l} \quad \forall i \quad (39)$$

The minimum storage capacity required to accommodate LNG received for each delivery ($Scur$) is calculated based on the volume unloaded by carriers (Uv), unloading frequencies (Fb and nl), and capacity margin (svr), as shown in Eq. (40). A similar approach is also used in Eqs. (41) and (42) to calculate storage requirements for local demand ($Scdr$) and for LNG deliveries to other locations ($Sclr$). These storage requirements are excluded for liquefaction plants, as their storage capacities are beyond the scope of this work.

$$svr \sum_c Uv_{r,c,i} \leq \sum_l Fb_{r,l} nl_l Scur_{r,i,l} \quad \forall r, i \notin il \quad (40)$$

$$svr \left(\sum_c Uv_{r,c,i} - \sum_{r,c} Lv_{r,c,i} \right) \leq \sum_l Fb_{r,l} nl_l Scdr_{r,i,l} \quad \forall r, i \notin il \quad (41)$$

$$svr \sum_c Lv_{r,c,i} \leq \sum_l Fb_{r,l} nl_l Sclr_{r,i,l} \quad \forall r, i \notin il \quad (42)$$

As observed, Eqs. (40)–(42) are non-linear due to bilinear terms. Their Glover's linearisation (Glover, 1975) forms, which are implemented in the model, are presented in Eqs. (43)–(48).

$$svr \sum_c Uv_{r,c,i} \leq \sum_l nl_l Scur_{r,i,l} \quad \forall r, i \quad (43)$$

$$Scur_{r,i,l} \leq Fb_{r,l} m \quad \forall r, c, l \quad (44)$$

$$svr \left(\sum_c Uv_{r,c,i} - \sum_{r,c} Lv_{r,c,i} \right) \leq \sum_l nl_l Scdr_{r,i,l} \quad \forall r, i \quad (45)$$

$$Scdr_{r,i,l} \leq Fb_{r,l} m \quad \forall r, i, l \quad (46)$$

$$svr \sum_c Lv_{r,c,i} \leq \sum_l nl_l Sclr_{r,i,l} \quad \forall r, i \quad (47)$$

$$Sclr_{r,i,l} \leq Fb_{r,l} m \quad \forall r, i, l \quad (48)$$

Finally, only one storage type (Sb) can be selected for each terminal (Eq. (49)), and the number of units that can be installed is specific to the storage type (Eq. (50)). For example, only one floating storage and regasification unit (FSRU) can be installed at each location, while multiple storage tanks can be installed at onshore facilities. These upper bounds are expressed as $nsrup$ in the equation.

$$\sum_s Sb_{i,s} \leq 1 \quad \forall i \quad (49)$$

$$Nsr_{i,s} \leq Sb_{i,s} nsrup_s \quad \forall i, s \quad (50)$$

2.3. Limitations

A range of criteria, such as environmental impact and risk/uncertainty factors, needs to be considered in supply chain designs (see Table 1). Although the proposed framework can be extended to incorporate those criteria in the system designs, this paper aims to demonstrate a proof of concept proposed in this framework in solving supply chain design problems. Therefore, to minimise the computational complexity of this study, several assumptions and simplifications are implemented in the framework.

1. This framework exclusively aims to minimise system cost. Other factors, such as emissions from shipping and land use for receiving terminals installation, which might be important in the 21st-century energy infrastructure development contexts, are not considered
2. In the case studies, LNG liquefaction plants are assumed to have unlimited supply, and the cost of storing LNG to ensure availability for carrier loading is not included in the FOB cost
3. This framework provides optimal solutions according to a single-period snapshot in the system. The case studies assume constant demand throughout the year and that the demand remains unchanged in future years. The integration of new nodes into the system and the removal of existing ones from it are not taken into account.
4. Terrain-related obstacles that may prevent certain types of carriers from accessing the port, such as shallow water and limited bridge clearance, are not considered. Similarly, additional infrastructure requirements, e.g., a jetty to enable access for carriers with deep draught in shallow water, are also not considered
5. The model is monopolistic; hence, the system is optimised according to the whole system's perspective without considering different and potentially conflicting objectives of different competitive actors in the system

Notwithstanding this, existing studies demonstrate the feasibility of incorporating environmental impacts, supply-side inventory constraints, and demand variability into supply chain models (Al-Haidous et al., 2022; Bittante and Saxén, 2020; Jokinen et al., 2015; Santos and Guedes Soares, 2024). Similarly, terrain-related obstacles can also be

readily incorporated into the framework by introducing relevant binary parameters and cost components. To capture conflicting objectives and potentially competitive behaviours among different actors in the system, a bi-level game approach, such as those presented in (Chalmardi and Camacho-Vallejo, 2019; Ramos et al., 2018, 2024), can be considered.

3. Case studies on small-scale LNG supply chain designs

In this work, the proposed framework for small-scale LNG supply chain design was applied to three case studies: the Maluku Islands, the Finnish coastline and the Caribbean Islands. These regions, illustrated in Fig. 3, differ substantially in terms of demand levels, distances between locations, and geographical contexts. These implementations aimed to demonstrate the framework's applicability across problems with differing characteristics. Following this, the effects of demand cluster sizes and supplier availability on system design and costs were analysed using the Maluku Islands case. Finally, the impacts of pre-determined shipping strategies and the separate sizing of shipping and storage on optimal solutions and costs were examined. This section presents data input and model setup to perform the analyses.

3.1. Data input

For the Maluku Islands case, the assumptions were based on the fact that Indonesia, as an archipelagic nation with thousands of small islands, has relied on oil-based power generation to meet the electricity demand in its small islands due to geographical constraints. However, the volatility of oil prices and growing environmental concerns prompted the government, through the state-owned electricity company (PLN), to phase out oil-based electricity in favour of cheaper natural gas-based power plants (PLN, 2021). Small-scale LNG systems can play a significant role in meeting the gas demand for these power plants. This is because offshore gas pipelines are generally more expensive for transporting gas over long distances to remote areas with small and dispersed demands.

Here, natural gas-based power plants are planned at 12 locations in the Maluku Islands, with gas supply expected from domestic sources, namely Tangguh- and the planned Abadi-LNG plants. To estimate the gas demand at each location, the planned capacity listed in the PLN's 10-year power sector expansion plan (PLN, 2021) is used, assuming all plants operate at an 80 % capacity factor and a heat rate of 11,370 Btu/kWh, which equates to a 30 % efficiency. Additionally, the heat



Fig. 3. Locations of terminals in the case studies. A) the Maluku Islands, B) the Finnish coastline, and C) the Caribbean Islands. Rectangles (□) and circles (○) represent liquefaction plants and demand locations, respectively. The size of each circle is proportional to the LNG demand, measured in thousands of cubic meters per year (TCM/y).

content of LNG from both locations is assumed to be equal at 23.6 MMBtu/m³ (IGU, 2024), priced at 8.24 USD/MMBtu (FOB). Table 2 outlines power plant capacity and LNG demand, along with the code name for each location. The distance between these locations can be seen in Fig. 4.

For the Finnish coastline and the Caribbean Islands cases, LNG demand and distance between locations data were adopted from (Jokinen et al., 2015; Bittante et al., 2018), respectively. These data can be seen in Table 3 and Fig. 5.

To deliver LNG to these locations, four types of carriers are considered. Although their average cruising speed is comparable, they vary by their carrying capacity, fuel consumption, loading-unloading rate, birthing time, and costs. Similarly, four storage options of different sizes are also considered. Between these storage types, only Tank-500 is allowed to be installed in multiple units within a single location of the receiving terminal. Other storage types are floating storage and regasification unit (FSRU), hence, rather than allowing multiple units to be installed in each location, different unit sizes of FSRU are provided as options. Key techno-economic parameters for the carriers and storage types considered are presented in Tables 4 and 5. In this study, LNG carriers can use gas from BOG formation as fuel, alongside MFO, which is priced at 17.06 USD/MMBtu.

3.2. Model setup

For the Maluku Islands case, 4 small-scale LNG supply chain models were developed using the proposed framework. These models vary in demand locations and LNG plants (suppliers) incorporated in each model, as outlined in Table 6. For the Finnish coastline and Caribbean Islands cases, separate models were developed, and their setups are presented in Table 7. The framework is implemented in GAMS 40.4.0, and all the models are solved using the CPLEX solver with a 0.00 % optimality gap on a computer with an Intel Core i7-1185G7 3 GHz processor and 16 GB of RAM, using 6 threads.

4. Results and discussion

4.1. Optimal shipping and receiving terminal designs

This section presents optimal small-scale LNG systems for the three regions in the Maluku Islands, the Finnish coastlines, and the Caribbean Islands, representing cases with different characteristics. Following this, the results for the Maluku Islands case are discussed to analyse how different modelling approaches influence the optimal system design. These discussions are outlined in the following sub-sections.

Table 2
Power plant capacities and LNG demand in the Maluku Islands.

Location	Code	Power Plant Capacity (MW)	Electricity Generated (GWh year ⁻¹)	Gas Demand (BBTU year ⁻¹)	LNG Demand, d_i (m ³ year ⁻¹)
Tangguh-LNG	TAN	–	–	–	–
Abadi-LNG	ABA	–	–	–	–
Ambon	AMB	170	1,191	13,546	573,973
Seram	SER	70	491	5,578	236,342
Namlea	NAM	30	210	2,390	101,289
Sanana	SAN	15	105	1,195	50,645
Ternate	TER	70	491	5,578	236,342
Tobelo	TOB	25	175	1,992	84,408
Bacan	BAC	10	70	797	33,763
Morotai	MOR	30	210	2,390	101,289
Langgur	LAN	20	140	1,594	67,526
Saumlaki	SAU	10	70	797	33,763
Dobo	DOB	20	140	1,594	67,526
Masela	MAS	20	140	1,594	67,526

4.1.1. Supply chain designs with endogenous logistics and storage size optimisation

Fig. 6 illustrates the optimal LNG shipping routes in the case studies. As can be seen in the figure, LNG from Tangguh-LNG is delivered to the receiving terminals in R1 using the milk-and-run approach. The route includes Bacan, Ternate, Morotai, and Tobelo, before returning to Tangguh-LNG to commence the next delivery cycle. To meet the region's demand, two C-5000 carriers are required. Using this strategy, each carrier completes 108 deliveries per year, with LNG stored in facilities sized at approximately 1/108 of local demand, ranging from 500 m³ in Bacan to 3500 m³ in Ternate, adjusted for the volume margin and storage unit sizes.

For R2, most gas demand is concentrated in Ambon (60 %) and Seram (25 %), which are close to Tangguh-LNG. In contrast, Namlea and Sanana, farther from Tangguh-LNG, account for only 11 % and 5 % of the R2 total demand, respectively. As a result, the shipping route is divided into 3 segments. As shown in Fig. 6, LNG is delivered directly from TAN to Seram using two units of C-1500 carrier and to Ambon using two units of C-5000 carrier. Here, Ambon serves as the hub to redistribute LNG to Namlea and Sanana by using a C-1500 carrier. These locations are visited 120 times annually, which is roughly every three days. For the Tangguh-Seram and Tangguh-Ambon routes, the carriers travel 180 and 168 times per year, respectively. Therefore, the storage volume requirements for their local demand are 3417 m³ for Ambon and 1313 m³ for Seram. Considering the unit volume of each storage type and the volume margin, Seram requires 4 units of Tank-500 storage. As an LNG hub, the design volume for the Ambon receiving terminal requires upsizing to accommodate not only storage requirements for the local demand but also additional LNG for redistribution to Namlea and Sanana. The results show that the Ambon terminal requires a unit of FSRU-7500 to cost-effectively satisfy these requirements.

LNG delivery from Tangguh-LNG to the R3 region involves 3 units of C-1500 carriers travelling to the receiving terminals 108 times annually. This requires 500 m³ of storage to be installed at Saumlaki and 1000 m³ at other locations in the region. In these results, the route is divided into two segments: Masela-Saumlaki and Langgur-Dobo. This is because Masela and Saumlaki are close to each other, as are Langgur and Dobo, while the two segments are far apart. Here, LNG from Tangguh is delivered to Masela and Saumlaki, after which the carrier returns to the LNG plant to reload its cargo before delivery to Langgur and Dobo.

While the supply from Tangguh is more certain, as the plant is already operational, the results show that the availability of Abadi-LNG may provide lower costs for the R3 region due to its proximity to the region's receiving terminals, assuming the same FOB price as Tangguh. The results of the R3-AT model provide insights into strategies if Abadi-LNG becomes available.

As shown in Fig. 6B, the shipping routes for R3 under the R3-AT model resemble the results in the R3-T setup. Here, Masela and Saumlaki are clustered separately from the Langgur-Dobo segment, and carriers return to Abadi-LNG after delivering LNG to Saumlaki and Masela before continuing to the Langgur-Dobo delivery. Using 2 units of C-1500 carriers, the system requires 108 deliverables per year to meet the annual demand in region R3 under the R3-AT setup.

For the Finnish coastline case, Fig. 6C shows that two shipping routes are selected. The main route employs three C-5000 carriers, each travelling 40 times a year, to transport LNG from Inkoo to Turku. After unloading, the carriers return to Inkoo for refilling before continuing their deliveries to Vaasa, Raahe, Tornio, and Oulu. To store the LNG, FSRU-7500 units are selected for Tornio and Turku, while Vaasa, Raahe, and Oulu use the Tank-500. As can be seen in the figure, the second route is dedicated to LNG delivery to Pori and employs a C-1500 carrier, travelling 180 times per year from Turku, which serves as the LNG hub for this route.

LNG demands in the Caribbean Islands are concentrated in the Dominican Republic and Puerto Rico, which account for 83 % of the LNG demand in the islands. Among these demand locations, only the

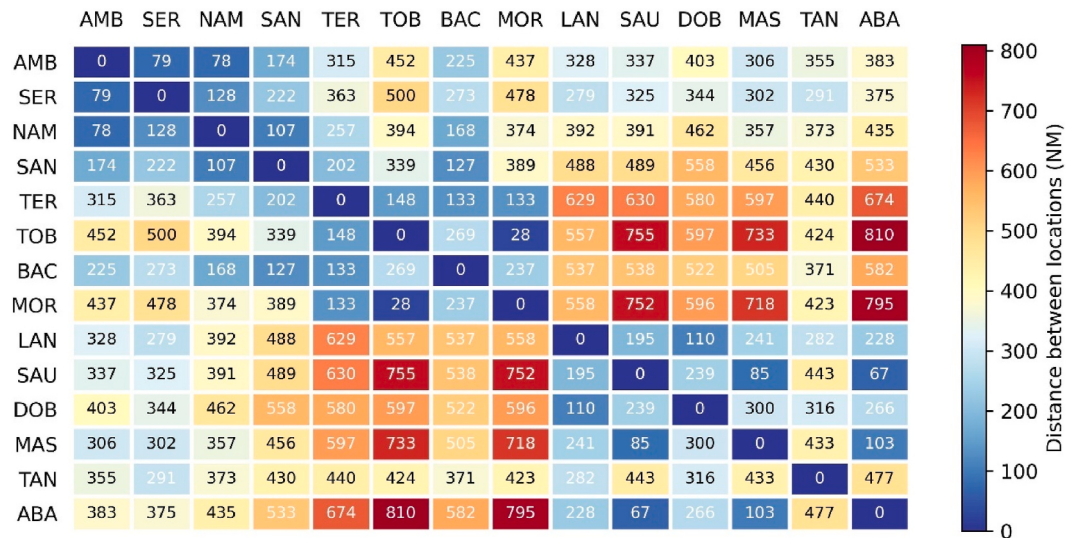


Fig. 4. Distance between locations in the Maluku Islands case.

Table 3

LNG demand in the Finnish coastline and the Caribbean Islands cases.

Location	Code	LNG Demand, d_i ($\text{m}^3 \text{ year}^{-1}$)
The Finnish coastline		
Inkoo	INK	–
Turku	TUR	248,815
Pori	POR	234,524
Vaasa	VAA	26,806
Raahe	RAA	60,991
Oulu	OUL	130,662
Tornio	TOR	287,430
The Caribbean Islands		
Trinidad and Tobago	TNT	–
USA-Florida	FLO	–
The Bahamas	BAH	120,000
Jamaica	JAM	264,000
Haiti	HAI	216,000
Dominican Republic	DRP	1,800,000
Puerto Rico	PRO	1,200,000

Bahamas is closer to Florida than to Trinidad and Tobago. Accordingly, the results show that LNG from Florida is only cost-effective for the Bahamas, while Jamaica, Haiti, the Dominican Republic, and Puerto Rico will need to import their LNG from Trinidad and Tobago. As observed in Fig. 6, the point-to-point logistics scheme is employed for LNG delivery from Florida to the Bahamas, using C-1500 as the carrier

and Tank-500 as storage. In contrast, a combination of point-to-point and hub-and-spoke is selected for LNG delivery for the rest of the node locations in the region. Here, a C-12000 carrier is used to deliver LNG to the Dominican Republic and Puerto Rico, where a unit of FSRU-15000 is installed in each location. As illustrated in the Figure, Puerto Rico is selected to serve as a hub to redistribute LNG to Haiti and Jamaica.

The results presented above reveal that the optimal supply chain designs in all case studies tend to combine point-to-point, milk-and-run, and hub-and-spoke schemes, rather than relying on a one-size-fits-all approach. Here, the node selected as a hub was generally observed to have a relatively large demand compared to other locations, such as Ambon and Puerto Rico. However, this does not apply to all cases. In the Finnish coastline case, for example, Turku and Pori have comparable demand levels, yet Turku, which is closer to Inkoo, is selected as the hub. Similarly, despite having the highest demand, Tornio is not selected as a hub. These results suggest that it is not economical to designate a hub at a location furthest from the LNG plant, even if it has the largest demand. This is because doing so would increase the shipping requirements to redistribute the LNG from the hub to the final destinations. Interestingly, in the Caribbean Islands case, despite having both the largest demand and central location in the system, the Dominican Republic is not selected as a hub. Instead, the results show that Puerto Rico, which is the second largest, is selected. The results show that selecting Puerto Rico as the hub allows the carrier serving both locations to deliver a similar

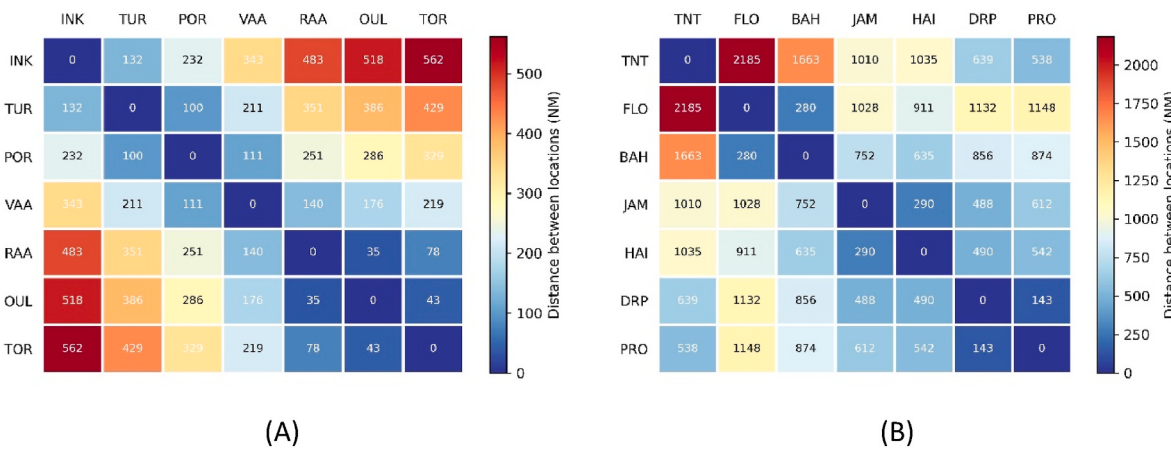


Fig. 5. Distance between locations. Data for A) the Finnish coastline and B) the Caribbean Islands cases.

Table 4
Carrier's techno-economic parameters.

Ship	Unit Capacity, ucc_c ($\text{m}^3 \text{ unit}^{-1}$)	Fuel Economy, fec_c (MMBtu NM $^{-1}$)	Voyage Speed, vc_c (knot)	Loading and Unloading Rate, $lurc_c$ ($\text{m}^3 \text{ hr}^{-1}$)	Berthing Time, btc_c (hr trip $^{-1}$)	Capital Expenditure, $capexc_c$ (Million \$ unit $^{-1}$)
C-1500	1,500	1.30	10	500	6	10.31
C-5000	5,000	2.88	10	1000	6	23.95
C-12000	12,000	3.41	10	1000	20	44.21
C-16500	16,500	3.91	10	1500	20	55.25

Table 5
Storage's techno-economic parameters.

Storage	Unit Capacity, ucs_s ($\text{m}^3 \text{ unit}^{-1}$)	Capital Expenditure of Storage, $capex_s$ (Million USD unit $^{-1}$)	Capital Expenditure of Non-storage, $capexns_s$ (USD $\text{m}^{-3} \text{ year}^{-1}$)
Tank-500	500	0.75	170
FSRU-7500	7,500	27.05	90
FSRU-15000	15,000	43.93	90
FSRU-22500	22,500	58.33	90

volume of LNG to each location, in which the excess LNG delivered to Puerto Rico is then redistributed to Haiti and Jamaica.

4.1.2. Impact of supply chain optimisation approaches

As discussed earlier, existing modelling frameworks and approaches in the literature often simplify the model by exogenously assuming shipping routes or logistic schemes. Furthermore, many studies also treat the storage size planning at receiving terminals separately from the optimisation of shipping strategy. However, the results from the models above show that shipping routes, which affect delivery frequency, and storage sizes are strongly correlated. It is therefore instructive to consider how these simplified approaches compare in terms of shipping routes, storage capacities, and costs when implemented in the regions.

In performing these analyses, the LNG-SCiPE framework was employed across all models for the Maluku Islands, *i.e.*, R1-T, R2-T, and R3-T. To examine the impact of the exogenous logistics scheme approach, each model was solved by restricting the solution to the milk-and-run scheme. This scheme was selected as the test case because it is among the most frequently predetermined assumptions in the literature (see Table 1). To quantify the impact of separating storage size planning from shipping, the process was divided into two steps. First, each model was run by setting zero costs at the receiving terminals. In this step, the supply chain was therefore designed to minimise the costs of gas and

carriers, without accounting for the costs associated with receiving terminal investments and operations. Second, the model was run with full techno-economic assumptions, including cost parameters for the receiving terminals. Results from the first step, *i.e.*, hub locations, shipping routes, and the number and type of carriers assigned to each route, were used to fix the values of these variables in the second step. Therefore, the designs of receiving terminals are optimised separately according to the pre-optimised shipping strategy.

Fig. 7A illustrates the results of optimisation using the milk-and-run logistics scheme across R1-T, R2-T, and R3-T models. For R1, the results align with those of the fully endogenous setup, which also identifies the milk-and-run scheme as the optimal strategy. In this calculation, however, the direction was inverted, indicating negligible cost differences, *i.e.*, within the optimality gap of 0.00 %, between the two options. For R2, however, the milk-and-run scheme requires carriers to deliver LNG more frequently, from 120 to 180 times in the fully endogenous setup, depending on the routes, to 228 times annually. Although this reduces the minimum storage capacity requirement at each terminal, the installed capacity remains the same due to the granularity of the storage unit size. Moreover, this strategy requires 4 units of C-5000 carriers, whereas the fully endogenous setup requires only 2 units of C-5000 and 3 units of C-1500 carriers. For R3, the milk-and-run scheme doubles the required frequency of delivery from 108 to 204 times annually. As a result, storage capacities at Langgur, Dobo, and Masela are reduced from 1000 m^3 to only 500 m^3 . However, to enable more frequent deliveries, the number of C-1500 carriers assigned for the region is increased from 3 to 4 units.

When shipping and receiving terminals are optimised separately, compared to the other setups, the resulting optimisation leads to significantly different shipping strategies in each of the models. As can be observed in Fig. 7B, Morotai serves as the hub for Tobelo, where the LNG in Morotai is delivered via the route of Tangguh–Morotai–Bacan–Tangguh–Ternate–Tangguh. Here, delivery frequency is reduced from 108 to 24 (main route) and 72 (Morotai – Tobelo route) times per year. This strategy minimises shipping costs by reducing operating expenses and harnessing economies of scale by using larger carriers (one unit of C-12000 and C-1500 each) rather than two units of C-5000. However, storage capacities increase significantly from 500–3500 m^3 to

Table 6
Regions represented in each small-scale LNG system model for the Maluku Islands case.

Model	LNG Plant		Receiving Terminal Cluster 1 (R1)				Receiving Terminal Cluster 2 (R2)				Receiving Terminal Cluster 3 (R3)			
	TAN	ABA	BAC	TER	MOR	TOB	SER	AMB	NAM	SAN	MAS	SAU	LAN	DOB
R1-T	O		O	O	O	O								
R2-T	O						O	O	O	O				
R3-T	O										O	O	O	O
R3-AT	O	O									O	O	O	O

Table 7
Regions represented in each small-scale LNG system model for the Finnish coastline and Caribbean Islands cases.

Model	Receiving Terminal – the Finnish coastline							Receiving Terminal – the Caribbean Islands								
	INK	TNT	FLO	TUR	RAU	POR	VAA	KOK	RAA	OUL	TOR	BAH	JAM	HAI	DRP	PRO
RFC	O			O	O	O	O	O	O	O	O					
RCI		O	O									O	O	O	O	O

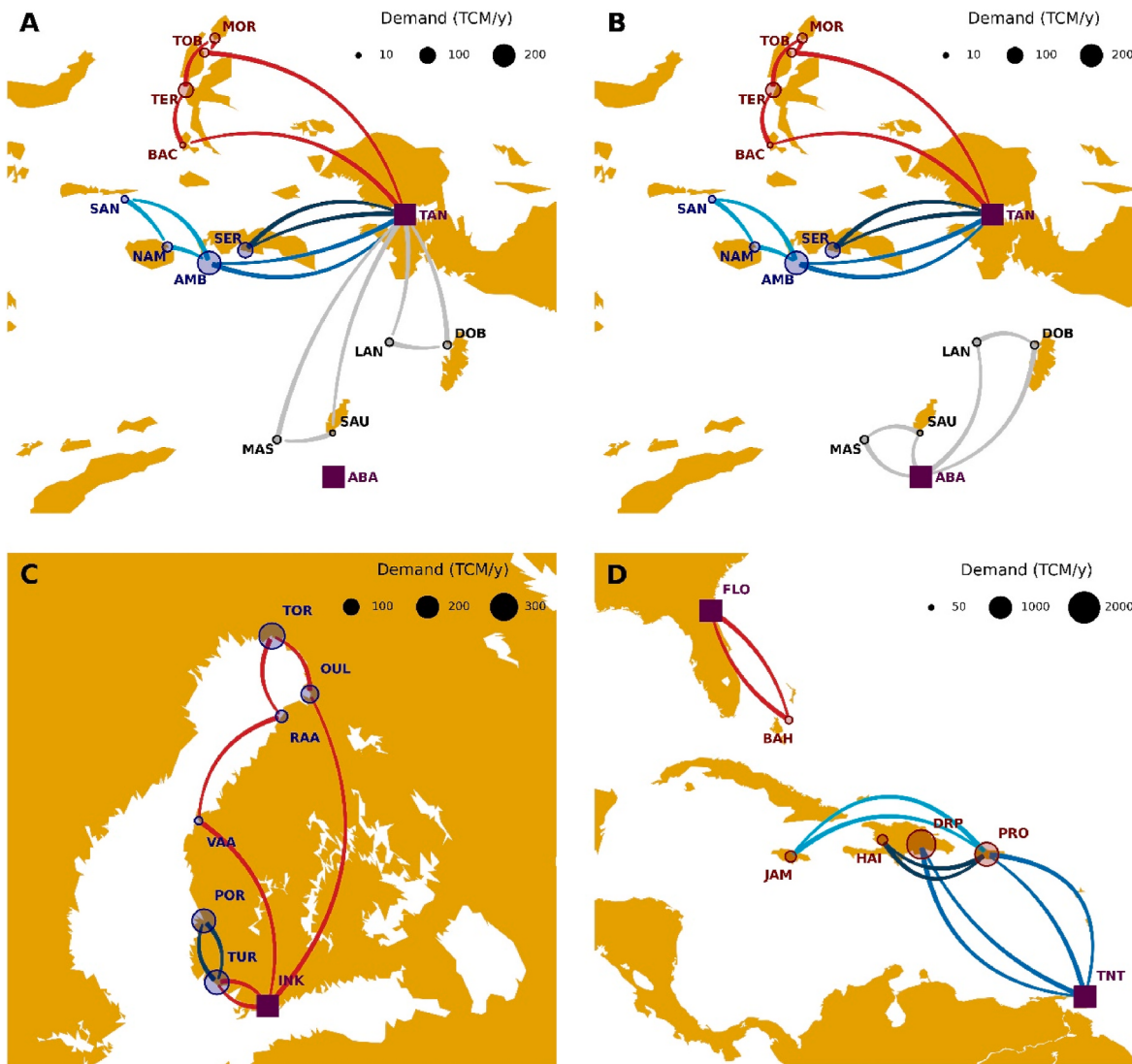


Fig. 6. Optimal shipping routes across different geographical contexts. A) the Maluku Islands with R1-T, R2-T, and R3-T models, B) the Maluku Islands with Abadi-LN availability, C) the Finnish coastlines, and D) the Caribbean Islands. The colours of the dots in A and B show receiving terminals at R1 (red), R2 (blue), and R3 (black). The colours of the lines distinguish the different shipping routes.

2000–15000 m³. Similar trends are also observed for R2 and R3.

Following these analyses, the approaches are also compared in terms of model complexity and solution time. As outlined in Table 8, the simplified approaches can reduce the number of variables in the model by 23–31 %. Similarly, the number of discrete variables is also decreased by around 5 %. Interestingly, solution time reductions significantly vary, ranging between 2 % in R2-T with separated shipping and storage optimisations and 99 % in R1-T with a pre-determined shipping strategy. Notwithstanding this, the longest solution time for the proposed approach application in these models is only 261 s.

4.2. The costs of delivered gas

In this section, the impacts of shipping and receiving terminal designs on costs are discussed. Total annual system costs, plant gate costs of natural gas, and the cost breakdowns are presented in Table 9. As can be observed, TASC is between 59 and 226 million USD/year. R2 has the highest total costs due to its large gas demand, while R3 has the lowest cost because of its smaller demand compared to other regions. Interestingly, the opposite trends are observed for the plant gate costs. As can be seen, the cost for R2 is the cheapest, i.e., 9.93 USD/MMBtu, followed by R1 at 10.36 USD/MMBtu. Finally, the cost for R3 is the most

expensive (10.59 USD/MMBtu). Interestingly, although Abadi-LNG has become available for the region, the cost remains more expensive than R2. For context, the distance between Tangguh-LNG and R2 is twice the distance between Abadi-LNG and R3. These results demonstrate that, to some extent, economies of scale have a stronger impact on costs than distance does. More detailed analyses of the impact of various factors on costs, including economies of scale and modelling approach, such as predetermined logistics schemes and separated optimisations of shipping and receiving terminals designs, are presented in the following subsections.

4.2.1. The role of economies of scale in small-scale LNG cost reductions

Reflecting on the results shown in Tables 9 and it is therefore instructive to quantify the role of the economies of scale effect in reducing the costs of the small-scale LNG supply chain. To perform this analysis, the number of terminals per region was varied from 1 to 12 (all locations). Details of these regional clusters can be seen in Table A1 in the appendix. The results of these experiments are presented in Fig. 8A, correlating shipping and receiving terminal costs in US cents/MMBtu·km with total annual gas demand, which corresponds to the number of demand locations incorporated in each demand cluster. Here, the shipping and receiving terminal costs are calculated by subtracting the

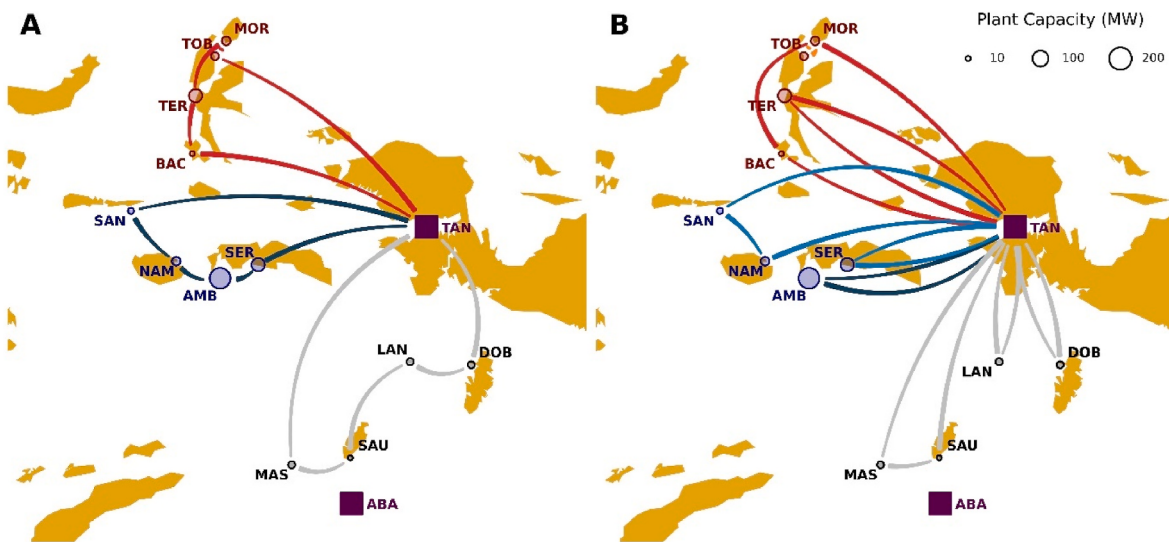


Fig. 7. Optimal shipping routes with simplified approaches. A) Optimal routes with the milk-and-run logistics scheme. B) Results of optimisation with separated shipping and receiving terminal optimisations.

Table 8

Model complexity and solution time comparison of different approaches. For the pre-determined shipping strategy approach, the milk-and-run scheme was used as the benchmark. For the separated shipping and storage optimisations, the first values are based on shipping optimisation (step 1). Values in the brackets are from storage optimisation (step 2).

Model	Proposed approach	Pre-determined shipping strategy	Separated shipping and storage optimisations
R1-T	No. of variables	20,876	16,068
	No. of discrete variables	292	276
	Solution time (seconds)	261.0	3.9
R2-T	No. of variables	20,876	16,068
	No. of discrete variables	292	276
	Solution time (seconds)	80.1	6.5
R3-T	No. of variables	20,876	16,068
	No. of discrete variables	292	276
	Solution time (seconds)	73.7	15.2
14,396 (2,280)			
276 (147)			
9.4 (1.2)			
14,396 (2,244)			
276 (140)			
77.2 (1.4)			
14,396 (2,624)			
276 (170)			
5.8 (1.1)			

FOB price of LNG at the liquefaction plant from the plant gate cost. This ensures that the costs of boil-off-gas (BOG) formations, which can be used as fuel for carriers, are captured. The obtained values are then adjusted based on the “distance analogue” between the LNG plant and the region. This distance analogue represents half of the shortest possible route that allows carriers to deliver LNG to each receiving terminal in the region exactly once and return to the LNG plant, as in the travelling salesman problem (Dantzig et al., 1954). As expected, the distance between the LNG plant and a single receiving terminal is half of the shortest possible route between the two locations.

The results show that total gas demand strongly affects shipping and receiving terminal costs, particularly when demand is below 500 BBtu

Table 9

Optimal system costs in each small-scale LNG supply chain model.

Model	Total Annual System Costs (TASC), Million USD year ⁻¹	Plant Gate Cost, USD MMBtu ⁻¹	Cost of Gas (CoG), USD MMBtu ⁻¹	Cost of Carrier (CoC), USD MMBtu ⁻¹	Cost of Receiving Terminal (CoR), USD MMBtu ⁻¹
R1-T	111	10.36	8.50	0.64	1.22
R2-T	226	9.93	8.43	0.50	1.00
R3-T	59	10.59	8.59	0.79	1.22
R3-AT	57	10.16	8.42	0.53	1.22

per year. As can be seen in the figure, increasing demand from 34 to 456 BBtu per year reduces the costs from 0.54 to 0.21 US cents/MMBtu-km, which corresponds to a 61 % reduction. Economies of scale analysis (Pratama et al., 2024) using the full dataset reveals an economies of scale parameter of 0.7, indicating that doubling the demand reduces costs by around 19 %. This factor is consistent with the parameter used to estimate the costs of carriers and storage of different sizes. Further increase in demand to 1650 BBtu per year results in further cost reductions to 1.5 US cents/MMBtu-km. It is important to note, however, that these costs are per kilometre, implying that there is a trade-off between demand size and distance analogue in determining the final plant gate cost, which is per MMBtu basis. Particularly, the marginal value of the economies of scale effect diminishes with demand size, while the impact of distance on cost is a linear function.

4.2.2. Framework with fully endogenous logistics schemes can reduce costs

In addition to economies of scale, the logistics scheme can also significantly affect costs. Fig. 8B compares breakdowns of plant gate costs between the fully endogenous and predetermined logistics schemes approach, using the milk-and-run as a case. As discussed in section 4.1, the approach with a predetermined milk-and-run scheme tends to increase delivery frequency, which might reduce storage installed capacity requirements. For R1, this approach does not affect costs, as the fully endogenous approach also indicates that the milk-and-run scheme is the optimal strategy. For R2, however, the milk-and-run scheme increases the shipping and receiving terminal costs by 8.3 % from 1.69 to 1.83 USD/MMBtu. The effect is the strongest in the R3 region with LNG supply from Abadi. As can be seen, the shipping and

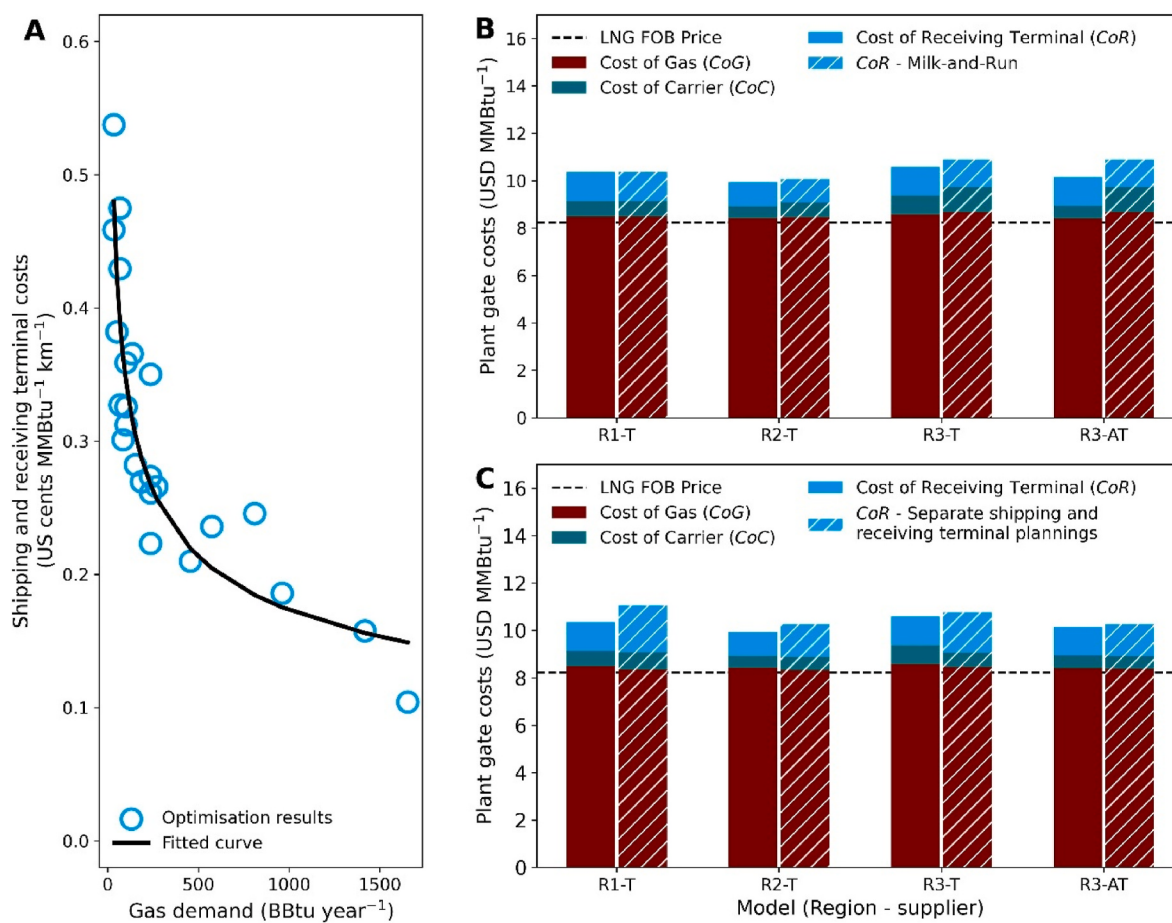


Fig. 8. Impact of different factors on the costs of gas delivered. A) Economies of scale, B) Predetermined logistics scheme (milk-and-run), and C) Separated shipping and receiving terminals optimisations.

receiving terminal costs increased by 38.5 %, from 1.92 to 2.66 USD/MMBtu. Under this setup, the cost of carriers doubles from 0.53 to 1.06 USD/MMBtu due to more frequent deliveries. Here, the milk-and-run scheme only decreases the cost of receiving terminals by 0.06 USD/MMBtu. These results show that allowing the framework to fully endogenously select optimal logistics schemes can substantially reduce costs.

4.2.3. Separated shipping and receiving terminal planning can significantly increase storage requirements at the receiving terminal

Finally, the results demonstrate that separating the optimisation of shipping and receiving terminals can lead to significant increases in receiving terminal costs. When receiving terminal design is excluded, the shipping design seeks to minimise costs by reducing travel frequency to lower fuel consumption and employing larger carriers to leverage on economies of scale. Compared to the complete framework, this approach reduces shipping costs by 0.03–0.30 USD/MMBtu. In R3 with Abadi supply, it does not reduce the cost of carriers but rather lowers the cost of gas by reducing BOG formation during travels. In R3 with supply from Tangguh, the savings become more noticeable. The cost of shipping decreases from 1.14 to 0.83 USD/MMBtu, contributed by 0.18 USD/MMBtu reductions in the cost of carrier and 0.13 USD/MMBtu of additional savings from BOG-related costs. Notwithstanding this, the plant gate cost modestly increases from 10.59 to 10.80 USD/MMBtu. This is driven by a considerable increase in the cost of receiving terminals from 1.22 to 1.70 USD/MMBtu. Compared to other regions, Fig. 8C illustrates that R1 is affected the most. As can be seen in the figure, shipping and receiving terminal costs increase from 2.12 to 2.83 USD/MMBtu. Here, the cost of receiving terminals increases by 62 %, negating the modest 6

% shipping cost reduction benefit from utilising larger carriers and less frequent delivery to the receiving terminals.

5. Conclusion

This paper presents a framework to optimise gas supply chain infrastructure planning, considering shipping fleet sizes, routes, and storage capacities at receiving terminals as decision variables. While existing works often rely on fixed logistics schemes, the proposed framework can identify optimal combinations of point-to-point, milk-and-run, and hub-and-spoke schemes, including optimal hub locations. Case studies in Indonesia's Maluku Islands, the Finnish coastline, and the Caribbean Islands were used to demonstrate its applicability across problems with diverse contexts. Several key conclusions can be drawn from the results, as outlined below.

- Simplified approaches, such as using predetermined shipping strategies or optimising shipping and receiving terminal capacities separately, can lead to suboptimal solutions as they can underestimate the cost implications of inefficient shipping strategies and storage designs. By treating shipping strategies as decision variables and simultaneously optimising shipping and storage designs, the proposed framework can provide substantially lower-cost solutions.
- Although the LNG hub in a hub-and-spoke scheme is typically located at the node with the highest local demand, this study reveals that additional factors, such as a node's relative distance to the LNG source and its impact on overall carrier utilisation, can play a significant role in determining the optimal hub location within the system.

- Increasing project sizes through demand clustering can substantially reduce costs. However, the marginal gains from these economies of scale quickly diminish as shipping distances increase. This underscores the significance of supply chain modelling and optimisation frameworks in quantifying the trade-offs between these factors to reduce costs.
- This framework relies on an MILP approach, which, although desirable to guarantee global optimal solutions, can become computationally expensive as problem size increases. For application in large problems, future work should explore approaches to decompose the problems into smaller sub-problems that can be solved more efficiently using the proposed framework (Garcia and You, 2015). Potential methods include a range of clustering algorithms (El Ouadi et al., 2022; Xu and Tian, 2015; Yunusoglu et al., 2024) and heuristic algorithm approaches (Bai and Fan, 2023; Nugroho et al., 2023; Zheng et al., 2020).

Nomenclature

Subscript	
<i>i</i>	node location index for terminals
<i>r</i>	route identifiers
<i>c</i>	carrier types
<i>l</i>	segments for travel frequency
<i>s</i>	storage types
<i>i, j, k</i>	aliases for terminal node locations
<i>il</i>	node location index for LNG plant terminal locations, where $il \in i$

Positive variables	
TASC	total annual system cost
CoG	cost of gas purchase from liquefaction terminal
CoC	cost of carrier
CoR	cost of receiving terminal
Bogy	volume of BOG formation
Lv	volume of LNG loaded to carrier
Rv	volume of LNG remains in carrier
Tv	volume of LNG transported by carrier
Uv	volume of LNG unloaded from carrier
Dec	marine fuel oil consumption by carrier
Fr	route's trip frequency in non-linear equation
Scr	storage capacity of receiving terminal
Scur	capacity needed to receive LNG
Scdr	capacity needed to store LNG for local demand
Sclr	capacity needed to store LNG for unloading to carriers
Tr	frequency of trips between node locations

Integer variables	
Nc	number of carriers operated
Nsr	number of storage tanks installed

Binary variables	
Cb	type of carriers
Fb	route's trip frequency in linearised equations
Hb	hub location
Rb	trip between node locations
Sb	storage type
Uvb	source of unloaded LNG

(continued on next column)

(continued)

Parameters	
avup	availability upper-bound
avlo	availability lower-bound
bi	availability of trips between node locations
btc	berthing time carrier
capexc	capital expenditures of carrier
capexs	capital expenditures of storage and FSRU
capexns	capital expenditures of receiving terminal's non-storage facility
cbogc	BOG formation rate coefficient
cgr	cost of gas regasification
crfc	cost recovery factor for carrier
crfr	cost recovery factor for receiving terminal
d	LNG demand
di	distance between locations
fec	fuel economy of carrier
fomc	fixed operating and maintenance factor of carrier
fomr	fixed operating and maintenance factor of receiving terminal
ghv	gross heating value of LNG
hvc	heel volume parameter of carriers
itcl0	minimum idle time
lurc	loading and unloading rates of carriers
m	any large number for the Glover's linearisation method
nl	frequency segment's parameter
pd	marine fuel oil price
pg	fixed on board (FOB) price of LNG
svr	storage capacity margin factor
ucc	unit capacity of carrier
ucs	unit capacity of storage
vc	speed of carrier

CRediT authorship contribution statement

Yoga Wienda Pratama: Writing – review & editing, Writing – original draft, Visualization, Validation, Software, Resources, Methodology, Investigation, Formal analysis, Data curation, Conceptualization. **Nadhilah Reyseliani:** Writing – review & editing. **Widodo Wahyu Purwanto:** Writing – review & editing, Resources, Methodology, Data curation.

Funding sources

This research did not receive any specific grant from funding agencies in the public, commercial, or not-for-profit sectors.

Declaration of competing interest

The authors declare the following financial interests/personal relationships which may be considered as potential competing interests: W.W.P. is currently serving as an Associate Editor in Gas Science and Engineering If there are other authors, they declare that they have no known competing financial interests or personal relationships that could have appeared to influence the work reported in this paper.

Appendix A

In this appendix, the regions represented in each model in the economies of scale analysis are presented in Table A1. As can be seen in the table, the main models, i.e., the R1-T, R2-T, R3-T, and R3-AT, are further divided into smaller regions, each comprising one or two demand locations. Additionally, the R12-T model was developed by combining the R1 and R2 regions, while the R123-T includes all demand locations in the analysis, with Tangguh-LNG designated as the LNG source. Due to model complexity, the R12-T and R123-T models were solved with a 5.00 % optimality gap.

Table A1

Regions represented in each model for economies-of-scale analysis

Model	LNG Plant		Receiving Terminal Cluster 1 (R1)				Receiving Terminal Cluster 2 (R2)				Receiving Terminal Cluster 3 (R3)			
	TAN	ABA	BAC	TER	MOR	TOB	SER	AMB	NAM	SAN	MAS	SAU	LAN	DOB
R1-T	O		O	O	O	O								
R1-T_BAC	O		O											
R1-T_TER	O			O										
R1-T_MOR	O				O									
R1-T_TOB	O					O								
R1-T_TER-BAC	O		O	O										
R1-T_MOR-TOB	O				O	O								
R2-T	O						O	O	O	O				
R2-T_SER	O						O							
R2-T_AMB	O							O						
R2-T_NAM	O								O					
R2-T_SAN	O									O				
R2-T_AMB-SER	O						O	O						
R2-T_SAN-NAM	O							O	O					
R3-T	O										O	O	O	O
R3-T_MAS	O										O			
R3-T_SAU	O											O		
R3-T_LAN	O												O	
R3-T_DOB	O													O
R3-T_MAS-SAU	O										O	O		
R3-T_LAN-DOB	O												O	O
R3-AT	O	O									O	O	O	O
R12-T	O		O	O	O	O	O	O	O	O				
R123-T	O		O	O	O	O	O	O	O	O	O	O	O	O

Data availability

Data will be made available on request.

References

- Abdullah, H.N., Artana, K.B., Dinariyana, A.A.B., Handani, D.W., Aprilia, P.W., 2021. Study on the LNG distribution to Bali – Nusa Tenggara power plants utilizing mini LNG carriers. IOP Conf. Ser. Mater. Sci. Eng. 1052, 012055. <https://doi.org/10.1088/1757-899X/1052/1/012055>.
- Abdullah, H.N., Artana, K.B., Zakaria, M.I., 2024. Techno-economic and supply chain model of a small-scale LNG for BMPP in Sambelia. IOP Conf. Ser. Earth Environ. Sci. 1423, 012020. <https://doi.org/10.1088/1755-1315/1423/1/012020>.
- Abdin, Z., 2024. Bridging the energy future: the role and potential of hydrogen co-firing with natural gas. J. Clean. Prod. 436, 140724. <https://doi.org/10.1016/j.jclepro.2024.140724>.
- Al-Haidous, S., Govindan, R., Elomri, A., Al-Ansari, T., 2022. An optimization approach to increasing sustainability and enhancing resilience against environmental constraints in LNG supply chains: a Qatar case study. Energy Rep. 8, 9742–9756. <https://doi.org/10.1016/j.egyr.2022.07.120>.
- Bai, B., Fan, W., 2023. Research on strategic liner ship fleet planning with regard to hub-and-spoke network. Oper. Manag. Res. 16, 363–376. <https://doi.org/10.1007/s12063-022-00315-2>.
- Bittante, A., Pettersson, F., Saxén, H., 2018. Optimization of a small-scale LNG supply chain. Energy 148, 79–89. <https://doi.org/10.1016/j.energy.2018.01.120>.
- Bittante, A., Saxén, H., 2020. Design of small LNG supply chain by multi-period optimization. Energies 13, 6704. <https://doi.org/10.3390/en13246704>.
- Budiyanto, M.A., Pamitran, A.S., Yusman, T., 2019. Optimization of the route of distribution of LNG using small scale LNG carrier: a case study of a gas power plant in the Sumatra Region, Indonesia. Int. J. Energy Econ. Policy 9, 179–187. <https://doi.org/10.32479/ijEEP.8103>.
- Budiyanto, M.A., Riadi, A., Buana, I.G.N.S., Kurnia, G., 2020. Study on the LNG distribution to mobile power plants utilizing small-scale LNG carriers. Heliyon 6, e04538. <https://doi.org/10.1016/j.heliyon.2020.e04538>.
- Budiyanto, M.A., Singgih, I.K., Riadi, A., Putra, G.L., 2022. Study on the LNG distribution to Mobile power plants using a Small-Scale LNG carrier for the case of the Sulawesi region of Indonesia. Energy Rep. 8, 374–380. <https://doi.org/10.1016/j.egyr.2021.11.211>.
- Bugaje, A.A.B., Dioha, M.O., Abraham-Dukuma, M.C., Wakil, M., 2022. Rethinking the position of natural gas in a low-carbon energy transition. Energy Res. Soc. Sci. 90, 102604. <https://doi.org/10.1016/j.erss.2022.102604>.
- Chalmardi, M.K., Camacho-Vallejo, J.-F., 2019. A bi-level programming model for sustainable supply chain network design that considers incentives for using cleaner technologies. J. Clean. Prod. 213, 1035–1050. <https://doi.org/10.1016/j.jclepro.2018.12.197>.
- Dantzig, G., Fulkerson, R., Johnson, S., 1954. Solution of a large-scale traveling-salesman problem. J. Oper. Res. Soc. Am. 2, 393–410. <https://doi.org/10.1287/opre.2.4.393>.
- Doymus, M., Sakar, G.D., Yildiz, S.T., Acik, A., 2022. Small-scale LNG supply chain optimization for LNG bunkering in Turkey. Comput. Chem. Eng. 162, 107789. <https://doi.org/10.1016/j.compchemeng.2022.107789>.
- El Ouadi, J., Malhene, N., Benhadou, S., Medromi, H., 2022. Towards a machine-learning based approach for splitting cities in freight logistics context: benchmarks of clustering and prediction models. Comput. Ind. Eng. 166, 107975. <https://doi.org/10.1016/j.cie.2022.107975>.
- Eriksen, U., Kristiansen, J., Fagerholt, K., Pantuso, G., 2022. Planning a maritime supply chain for liquefied natural gas under uncertainty. Marit. Transp. Res. 3, 100061. <https://doi.org/10.1016/j.marta.2022.100061>.
- Fauzi, I., Ispandiari, A.R., 2024. Green LNG supply chain: optimizing distribution in eastern Indonesia. Evergreen 11, 2624–2637. <https://doi.org/10.5109/7236902>.
- Faydi, Y., Djidua, A., Laabassi, H., Omar, A.A., Bouzekri, H., 2024. Contribution of green hydrogen vector to guarantee electricity feeding in remote areas- case study. Renew. Energy 222, 119880. <https://doi.org/10.1016/j.renene.2023.119880>.
- Fescioglu-Unver, N., Aktaş, M.Y., 2023. Electric vehicle charging service operations: a review of machine learning applications for infrastructure planning, control, pricing and routing. Renew. Sustain. Energy Rev. 188, 113873. <https://doi.org/10.1016/j.rser.2023.113873>.
- Garcia, D.J., You, F., 2015. Supply chain design and optimization: challenges and opportunities. Comput. Chem. Eng. 81, 153–170. <https://doi.org/10.1016/j.compchemeng.2015.03.015>.
- Glover, F., 1975. Improved linear integer programming formulations of nonlinear integer problems. Manag. Sci. 22, 455–460. <https://doi.org/10.1287/mnsc.22.4.455>.
- Hadi, F., Supomo, H., Achmadi, T., 2023. Using genetic algorithm for fleet assignment of small-scale LNG supply chain. IOP Conf. Ser. Earth Environ. Sci. 1166, 012045. <https://doi.org/10.1088/1755-1315/1166/1/012045>.
- IGU, 2024. 2024 World LNG Report. International Gas Union (IGU). London.
- Intergovernmental Panel on Climate Change (IPCC), 2023. In: Climate Change 2022 - Mitigation of Climate Change: Working Group III Contribution to the Sixth Assessment Report of the Intergovernmental Panel on Climate Change, first ed. Cambridge University Press. <https://doi.org/10.1017/9781009157926>.
- Jokinen, R., Pettersson, F., Saxén, H., 2015. An MILP model for optimization of a small-scale LNG supply chain along a coastline. Appl. Energy 138, 423–431. <https://doi.org/10.1016/j.apenergy.2014.10.039>.
- Konstantakopoulos, G.D., Gayialis, S.P., Kechagias, E.P., 2022. Vehicle routing problem and related algorithms for logistics distribution: a literature review and classification. Oper. Res. 22, 2033–2062. <https://doi.org/10.1007/s12351-020-00600-7>.
- Machfudiyanto, R.A., Muslim, F., Humang, W.P., Wahjuningsih, N., Kamil, I., Ichsan, M., Putra, Y.Y.A., 2023. Optimization of the risk-based small-scale LNG supply chain in the Indonesian archipelago. Heliyon 9, e19047. <https://doi.org/10.1016/j.heliyon.2023.e19047>.
- Neksa, P., Brendeng, E., Drescher, M., Norberg, B., 2010. Development and analysis of a natural gas liquefaction plant for small gas carriers. J. Nat. Gas Sci. Eng. 2, 143–149. <https://doi.org/10.1016/j.jngse.2010.05.001>.
- Nugroho, A.C.P.T., Hakim, B.A., Hendrik, D., Sasmito, C., Muttaqie, T., Tjolleng, A., Iskendar, Kurniawan, M.A., Komariyah, S., 2023. Mission analysis of small-scale LNG

- carrier as feeder for east Indonesia: ambon city as the hub terminal. Evergreen 10, 1938–1950. <https://doi.org/10.5109/7151748>.
- Olabi, A.G., Abdelkareem, M.A., Mahmoud, M.S., Elsaied, K., Obaideen, K., Rezk, H., Wilberforce, T., Eisa, T., Chae, K.-J., Sayed, E.T., 2023. Green hydrogen: pathways, roadmap, and role in achieving sustainable development goals. *Process Saf. Environ. Prot.* 177, 664–687. <https://doi.org/10.1016/j.psep.2023.06.069>.
- Papaleonidas, C., Lyridis, D.V., Papakostas, A., Konstantinidis, D.A., 2020. An innovative decision support tool for liquefied natural gas supply chain planning. *Marit. Bus. Rev.* 5, 121–136. <https://doi.org/10.1108/MABR-09-2019-0036>.
- PLN, 2021. Rencana Usaha Penyediaan Tenaga Listrik (RUPTL) 2021–2030. Perusahaan Listrik Negara (PLN), Jakarta.
- Pratama, Y.W., Gidden, M.J., Greene, J., Zaiser, A., Nemet, G., Riahi, K., 2024. Learning, economies of scale, and knowledge gap effects on power generation technology cost improvements. *iScience*, 111644. <https://doi.org/10.1016/j.isci.2024.111644>.
- Pratama, Y.W., Mac Dowell, N., 2022. Carbon capture and storage investment: fiddling while the planet burns. *One Earth* 5, 434–442. <https://doi.org/10.1016/j.oneear.2022.03.008>.
- Pratama, Y.W., Purwanto, W.W., Tezuka, T., McLellan, B.C., Hartono, D., Hidayatno, A., Daud, Y., 2017. Multi-objective optimization of a multiregional electricity system in an archipelagic state: the role of renewable energy in energy system sustainability. *Renew. Sustain. Energy Rev.* 77, 423–439. <https://doi.org/10.1016/j.rser.2017.04.021>.
- Pratiwi, E., Handani, D.W., Antara, G.B.D.S., Dinariyana, A.A.B., Abdillah, H.N., 2021. Economic analysis on the LNG distribution to power plants in Bali and lombok by utilizing mini-LNG carriers. *IOP Conf. Ser. Mater. Sci. Eng.* 1052, 012053. <https://doi.org/10.1088/1757-899X/1052/1/012053>.
- Ramos, M.A., Boix, M., Aussel, D., Montastruc, L., 2024. Development of a multi-leader multi-follower game to design industrial symbioses. *Comput. Chem. Eng.* 183, 108598. <https://doi.org/10.1016/j.compchemeng.2024.108598>.
- Ramos, M.A., Rocafull, M., Boix, M., Aussel, D., Montastruc, L., Domenech, S., 2018. Utility network optimization in eco-industrial parks by a multi-leader follower game methodology. *Comput. Chem. Eng.* 112, 132–153. <https://doi.org/10.1016/j.compchemeng.2018.01.024>.
- Ratnakar, R.R., Gupta, N., Zhang, K., Van Doorn, C., Fesmire, J., Dindoruk, B., Balakotaiah, V., 2021. Hydrogen supply chain and challenges in large-scale LH₂ storage and transportation. *Int. J. Hydrol. Energy* 46, 24149–24168. <https://doi.org/10.1016/j.ijhydene.2021.05.025>.
- Raza, M.Y., Lin, B., 2022. Natural gas consumption, energy efficiency and low carbon transition in Pakistan. *Energy* 240, 122497. <https://doi.org/10.1016/j.energy.2021.122497>.
- Reyseliani, N., Pratama, Y.W., Hidayatno, A., Mac Dowell, N., Purwanto, W.W., 2024. Power sector decarbonisation in developing and coal-producing countries: a case study of Indonesia. *J. Clean. Prod.* 454, 142202. <https://doi.org/10.1016/j.jclepro.2024.142202>.
- Santos, A.M.P., Guedes Soares, C., 2024. Cost optimization of shuttle tanker offloading operations. *Ocean Eng* 301, 117378. <https://doi.org/10.1016/j.oceaneng.2024.117378>.
- Sommeng, A.N., Usman, U., Kurnianto, J., 2023. Techno-economic and risk assessment of small-scale LNG distribution for replacing diesel fuel in nusa Tenggara region. *Int. J. Energy Econ. Policy* 13, 356–364. <https://doi.org/10.32479/ijEEP.14446>.
- Spatoliso, E., Restelli, F., Pellegrini, L.A., Cattaneo, S., De Angelis, A.R., Lainati, A., Roccaro, E., 2024. Liquefied hydrogen, ammonia and liquid organic hydrogen carriers for harbour-to-harbour hydrogen transport: a sensitivity study. *Int. J. Hydrol. Energy* 80, 1424–1431. <https://doi.org/10.1016/j.ijhydene.2024.07.241>.
- Strantzali, E., Aravossis, K., Livanos, G., Chrysanthopoulos, N., 2018. A novel multicriteria evaluation of small-scale LNG supply alternatives: the case of Greece. *Energies* 11, 903. <https://doi.org/10.3390/en11040903>.
- Xu, D., Tian, Y., 2015. A comprehensive survey of clustering algorithms. *Ann. Data Sci.* 2, 165–193. <https://doi.org/10.1007/s40745-015-0040-1>.
- Yunusoglu, P., Ozsoydan, F.B., Bilgen, B., 2024. A machine learning-based two-stage approach for the location of undesirable facilities in the biomass-to-bioenergy supply chain. *Appl. Energy* 362, 122961. <https://doi.org/10.1016/j.apenergy.2024.122961>.
- Zheng, M., Li, W., Liu, Y., Liu, X., 2020. A Lagrangian heuristic algorithm for sustainable supply chain network considering CO₂ emission. *J. Clean. Prod.* 270, 122409. <https://doi.org/10.1016/j.jclepro.2020.122409>.